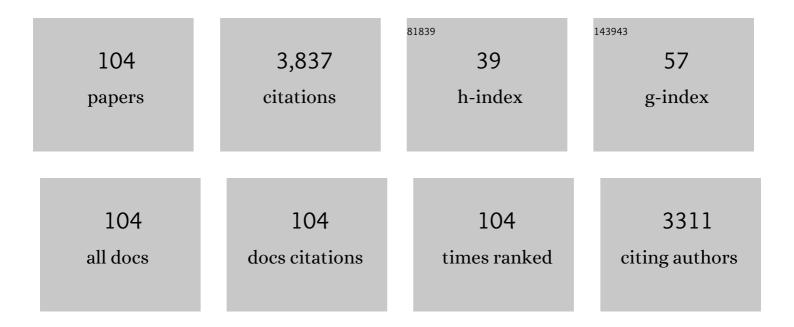
Xidong Wang

List of Publications by Year in descending order

Source: https://exaly.com/author-pdf/11041717/publications.pdf Version: 2024-02-01



#	Article	IF	CITATIONS
1	Density-controlled hydrothermal growth of well-aligned ZnO nanorod arrays. Nanotechnology, 2007, 18, 035605.	1.3	169
2	In situ DRIFTS investigation on the SCR of NO with NH3 over V2O5 catalyst supported by activated semi-coke. Applied Surface Science, 2014, 313, 660-669.	3.1	145
3	Environmental investigation on co-combustion of sewage sludge and coal gangue: SO 2 , NO x and trace elements emissions. Waste Management, 2016, 50, 213-221.	3.7	108
4	Promoting effect of Nd on the reduction of NO with NH ₃ over CeO ₂ supported by activated semi-coke: an in situ DRIFTS study. Catalysis Science and Technology, 2015, 5, 2251-2259.	2.1	105
5	FTIR, Raman and NMR investigation of CaO–SiO2–P2O5 and CaO–SiO2–TiO2–P2O5 glasses. Journal o Non-Crystalline Solids, 2015, 420, 26-33.	f _{1.5}	102
6	Investigation of the Viscosity and Structural Properties of CaO-SiO2-TiO2 Slags. Metallurgical and Materials Transactions B: Process Metallurgy and Materials Processing Science, 2014, 45, 1389-1397.	1.0	99
7	Hydrothermal synthesis and characterization of TiO2 nanorod arrays on glass substrates. Materials Research Bulletin, 2009, 44, 1232-1237.	2.7	98
8	Effect of Al ₂ 0 ₃ /SiO ₂ Ratio on the Viscosity and Structure of Slags. ISIJ International, 2012, 52, 753-758.	0.6	90
9	Recycling of municipal solid waste incineration by-product for cement composites preparation. Construction and Building Materials, 2018, 162, 794-801.	3.2	84
10	Heat Recovery from High Temperature Slags: A Review of Chemical Methods. Energies, 2015, 8, 1917-1935.	1.6	83
11	Raman spectroscopic study of the structural properties of CaO–MgO–SiO2–TiO2 slags. Journal of Non-Crystalline Solids, 2013, 376, 209-215.	1.5	79
12	Activated Semi-coke in SO ₂ Removal from Flue Gas: Selection of Activation Methodology and Desulfurization Mechanism Study. Energy & Fuels, 2013, 27, 3080-3089.	2.5	78
13	Low-temperature SCR of NO with NH3 over activated semi-coke composite-supported rare earth oxides. Applied Surface Science, 2014, 309, 1-10.	3.1	71
14	In situ DRIFTS studies on MnO nanowires supported by activated semi-coke for low temperature selective catalytic reduction of NO with NH3. Applied Surface Science, 2016, 366, 139-147.	3.1	71
15	Electrochemical deposition of branched hierarchical ZnO nanowire arrays and its photoelectrochemical properties. Electrochimica Acta, 2011, 56, 5776-5782.	2.6	68
16	Synthesis, characterization and modeling of new building insulation material using ceramic polishing waste residue. Construction and Building Materials, 2015, 85, 119-126.	3.2	63
17	Effects of preparing conditions on the electrodeposition of well-aligned ZnO nanorod arrays. Electrochimica Acta, 2008, 53, 4633-4641.	2.6	62
18	Effect of water-washing on the co-removal of chlorine and heavy metals in air pollution control residue from MSW incineration. Waste Management, 2017, 68, 221-231.	3.7	62

#	Article	IF	CITATIONS
19	Synthesis of a foam ceramic based on ceramic tile polishing waste using SiC as foaming agent. Ceramics International, 2018, 44, 10078-10086.	2.3	62
20	Experimental investigation and modeling of cooling processes of high temperature slags. Energy, 2014, 76, 761-767.	4.5	61
21	Tailoring CoO–ZnO nanorod and nanotube arrays for Li-ion battery anode materials. Journal of Materials Chemistry A, 2013, 1, 9654.	5.2	59
22	Crystallization Behavior of Rutile in the Synthesized Ti-bearing Blast Furnace Slag Using Single Hot Thermocouple Technique. ISIJ International, 2011, 51, 1396-1402.	0.6	58
23	Insight into the Relationship Between Viscosity and Structure of CaO-SiO2-MgO-Al2O3 Molten Slags. Metallurgical and Materials Transactions B: Process Metallurgy and Materials Processing Science, 2019, 50, 2930-2941.	1.0	57
24	The Influence of SiO ₂ on the Extraction of Ti Element from Tiâ€bearing Blast Furnace Slag. Steel Research International, 2011, 82, 607-614.	1.0	55
25	Effect of B2O3 on the Structure and Viscous Behavior of Ti-Bearing Blast Furnace Slags. Jom, 2014, 66, 2168-2175.	0.9	55
26	Integrated utilization of high alumina fly ash for synthesis of foam glass ceramic. Ceramics International, 2018, 44, 13681-13688.	2.3	55
27	Reuse of mineral wool waste and recycled glass in ceramic foams. Ceramics International, 2019, 45, 15057-15064.	2.3	55
28	Pore size-controlled gases and alcohols separation within ultramicroporous homochiral lanthanide–organic frameworks. Journal of Materials Chemistry, 2012, 22, 7813.	6.7	53
29	Integrated carbon dioxide/sludge gasification using waste heat from hot slags: Syngas production and sulfur dioxide fixation. Bioresource Technology, 2015, 181, 174-182.	4.8	53
30	Influence of Basicity and TiO2 Content on the Precipitation Behavior of the Ti-bearing Blast Furnace Slags. ISIJ International, 2013, 53, 1696-1703.	0.6	50
31	Ultrasensitive sorption behavior of isostructural lanthanide–organic frameworks induced by lanthanide contraction. Journal of Materials Chemistry, 2012, 22, 21076.	6.7	48
32	Effects of chemistry and mineral on structural evolution and chemical reactivity of coal gangue during calcination: towards efficient utilization. Materials and Structures/Materiaux Et Constructions, 2015, 48, 2779-2793.	1.3	48
33	Preparation and characterization of permeable bricks from gangue and tailings. Construction and Building Materials, 2017, 148, 484-491.	3.2	47
34	Recycling ground MSWI bottom ash in cement composites: Long-term environmental impacts. Waste Management, 2018, 78, 841-848.	3.7	46
35	Hydrothermal Synthesis of CeO ₂ Nanoparticles on Activated Carbon with Enhanced Desulfurization Activity. Energy & Fuels, 2012, 26, 5879-5886.	2.5	45
36	Two-stage high temperature sludge gasification using the waste heat from hot blast furnace slags. Bioresource Technology, 2015, 198, 364-371.	4.8	45

#	Article	IF	CITATIONS
37	Correlation and Prediction of Activity and Osmotic Coefficients of Aqueous Electrolytes at 298.15 K by the Modified TCPC Model. Journal of Chemical & Engineering Data, 2007, 52, 538-547.	1.0	43
38	Multi-Stage Control of Waste Heat Recovery from High Temperature Slags Based on Time Temperature Transformation Curves. Energies, 2014, 7, 1673-1684.	1.6	42
39	Synthesis of a ceramic tile base based on high-alumina fly ash. Construction and Building Materials, 2017, 155, 930-938.	3.2	42
40	Hydrothermal growth of well-aligned TiO2 nanorod arrays: Dependence of morphology upon hydrothermal reaction conditions. Rare Metals, 2010, 29, 286-291.	3.6	40
41	Preparation of Slag Wool by Integrated Waste-Heat Recovery and Resource Recycling of Molten Blast Furnace Slags: From Fundamental to Industrial Application. Energies, 2014, 7, 3121-3135.	1.6	40
42	The Effect of P2O5 on the Crystallization Behaviors of Ti-Bearing Blast Furnace Slags Using Single Hot Thermocouple Technique. Metallurgical and Materials Transactions B: Process Metallurgy and Materials Processing Science, 2014, 45, 1446-1455.	1.0	40
43	Fabrication and characterization of porous cordierite ceramics prepared from fly ash and natural minerals. Ceramics International, 2019, 45, 18306-18314.	2.3	40
44	Characteristics of low temperature biomass gasification and syngas release behavior using hot slag. RSC Advances, 2014, 4, 62105-62114.	1.7	36
45	Estimation of Freezing Point Depression, Boiling Point Elevation, and Vaporization Enthalpies of Electrolyte Solutions. Industrial & Engineering Chemistry Research, 2009, 48, 2229-2235.	1.8	34
46	Integrated utilization of fly ash and waste glass for synthesis of foam/dense bi-layered insulation ceramic tile. Energy and Buildings, 2018, 168, 67-75.	3.1	32
47	Trace element partitioning behavior of coal gangue-fired CFB plant: experimental and equilibrium calculation. Environmental Science and Pollution Research, 2015, 22, 15469-15478.	2.7	29
48	Application of washed MSWI fly ash in cement composites: long-term environmental impacts. Environmental Science and Pollution Research, 2018, 25, 12127-12138.	2.7	29
49	Synthesis, evaluation and characterization of alumina ceramics with elongated grains. Ceramics International, 2005, 31, 953-958.	2.3	28
50	Pyrite transformation and sulfur dioxide release during calcination of coal gangue. RSC Advances, 2014, 4, 42506-42513.	1.7	27
51	Achieving waste to energy through sewage sludge gasification using hot slags: syngas production. Scientific Reports, 2015, 5, 11436.	1.6	27
52	Co-modification and Crystalline-control of Ti-bearing Blast Furnace Slags. ISIJ International, 2015, 55, 158-165.	0.6	25
53	Manganese oxide catalysts supported on zinc oxide nanorod arrays: A new composite for selective catalytic reduction of NOx with NH3 at low temperature. Applied Surface Science, 2019, 491, 579-589.	3.1	25
54	Integration of biomass/steam gasification with heat recovery from hot slags: Thermodynamic characteristics. International Journal of Hydrogen Energy, 2016, 41, 5916-5926.	3.8	24

#	Article	IF	CITATIONS
55	Thermodynamic study and synthesis of gamma-aluminum oxynitride. Scandinavian Journal of Metallurgy, 2002, 31, 1-6.	0.3	23
56	Effect of P2O5 Addition on the Viscosity and Structure of Titanium Bearing Blast Furnace Slags. ISIJ International, 2014, 54, 1491-1497.	0.6	23
57	Fuel nitrogen conversion and release of nitrogen oxides during coal gangue calcination. Environmental Science and Pollution Research, 2015, 22, 7139-7146.	2.7	23
58	Promotional effect of rare earth-doped manganese oxides supported on activated semi-coke for selective catalytic reduction of NO with NH3. Environmental Science and Pollution Research, 2017, 24, 24473-24484.	2.7	23
59	Correlation and Prediction of Thermodynamic Properties of Some Complex Aqueous Electrolytes by the Modified Three-Characteristic-Parameter Correlation Model. Journal of Chemical & Engineering Data, 2008, 53, 950-958.	1.0	22
60	Calculations of Freezing Point Depression, Boiling Point Elevation, Vapor Pressure and Enthalpies ofÂVaporization of Electrolyte Solutions by a Modified Three-Characteristic Parameter Correlation Model. Journal of Solution Chemistry, 2009, 38, 1097-1117.	0.6	22
61	Development of the random simulation model for estimating the effective thermal conductivity of insulation materials. Building and Environment, 2014, 80, 221-227.	3.0	21
62	Effect of Al2O3 Addition on the Precipitated Phase Transformation in Ti-Bearing Blast Furnace Slags. Metallurgical and Materials Transactions B: Process Metallurgy and Materials Processing Science, 2016, 47, 1390-1399.	1.0	21
63	Role of steel slags on biomass/carbon dioxide gasification integrated with recovery of high temperature heat. Bioresource Technology, 2017, 223, 1-9.	4.8	21
64	Effect of Substrate Pretreatment on Controllable Growth of TiO2 Nanorod Arrays. Journal of Materials Science and Technology, 2012, 28, 577-586.	5.6	20
65	Investigation on slag fiber characteristics: Mechanical property and anti-corrosion performance. Ceramics International, 2015, 41, 5677-5687.	2.3	20
66	Integration of coal gasification and waste heat recovery from high temperature steel slags: an emerging strategy to emission reduction. Scientific Reports, 2015, 5, 16591.	1.6	19
67	A Simple Two-Parameter Correlation Model for Aqueous Electrolyte Solutions across a Wide Range of Temperatures. Journal of Chemical & Engineering Data, 2009, 54, 179-186.	1.0	17
68	Facile and economical synthesis of porous activated semi-cokes for highly efficient and fast removal of microcystin-LR. Journal of Hazardous Materials, 2015, 299, 325-332.	6.5	17
69	Integrated Utilization of Sewage Sludge and Coal Gangue for Cement Clinker Products: Promoting Tricalcium Silicate Formation and Trace Elements Immobilization. Materials, 2016, 9, 275.	1.3	17
70	Integrated biomass gasification using the waste heat from hot slags: Control of syngas and polluting gas releases. Energy, 2016, 114, 165-176.	4.5	17
71	Ultralow loading of Cu2O/CuO nanoparticles on metal-organic framework-derived carbon octahedra and activated semi-coke for highly efficient SO2 removal. Journal of Cleaner Production, 2022, 341, 130823.	4.6	17
72	Estimation of viscosity of ternary-metallic melts. Metallurgical and Materials Transactions A: Physical Metallurgy and Materials Science, 2002, 33, 3201-3204.	1.1	16

#	Article	IF	CITATIONS
73	Kinetic studies of the oxidation of γ-aluminum oxynitride. Metallurgical and Materials Transactions B: Process Metallurgy and Materials Processing Science, 2002, 33, 201-207.	1.0	16
74	Correlation and Prediction of Thermodynamic Properties of Nonaqueous Electrolytes by the Modified TCPC Model. Journal of Chemical & Engineering Data, 2008, 53, 149-159.	1.0	16
75	Numerical modeling and experimental study of heat transfer in ceramic fiberboard. Textile Reseach Journal, 2014, 84, 411-421.	1.1	16
76	Roles of P ₂ O ₅ Addition on the Viscosity and Structure of CaO–SiO ₂ –Al ₂ O ₃ –Na _{ Melts. ISIJ International, 2018, 58, 1644-1649.}	2&l t)/s ub&ş	gt; O –P<s
77	Development of structure-informed artificial neural network for accurately modeling viscosity of multicomponent molten slags. Ceramics International, 2021, 47, 30691-30701.	2.3	16
78	Preparation and characterization of the one-piece wall ceramic board by using solid wastes. Ceramics International, 2017, 43, 8564-8571.	2.3	14
79	Kinetic studies of oxidation of γ-AlON–TiN composites. Journal of Alloys and Compounds, 2005, 387, 74-81.	2.8	12
80	A Novel Kinematic Model for Molten Slag Fiberization: Prediction of Slag Fiber Properties. Metallurgical and Materials Transactions B: Process Metallurgy and Materials Processing Science, 2015, 46, 993-1001.	1.0	12
81	ANN-based structure-viscosity relationship model of multicomponent slags for production design in mineral wool. Construction and Building Materials, 2022, 319, 126010.	3.2	12
82	A new three-particle-interaction model to predict the thermodynamic properties of different electrolytes. Journal of Chemical Thermodynamics, 2007, 39, 602-612.	1.0	11
83	Kinetic studies on bituminous coal char gasification using CO ₂ and H ₂ O mixtures. International Journal of Green Energy, 2019, 16, 1144-1151.	2.1	11
84	Preparation, Sintering Behavior and Consolidation Mechanism of Vanadium-Titanium Magnetite Pellets. Crystals, 2021, 11, 188.	1.0	11
85	Structural and Viscous Insight into Impact of MoO3 on Molten Slags. Metallurgical and Materials Transactions B: Process Metallurgy and Materials Processing Science, 2021, 52, 3730-3743.	1.0	11
86	Preparation and modeling of energy-saving building materials by using industrial solid waste. Energy and Buildings, 2015, 97, 6-12.	3.1	10
87	In Situ DRIFTS Investigation on CeOx Catalyst Supported by Fly-Ash-Made Porous Cordierite Ceramics for Low-Temperature NH3-SCR of NOX. Catalysts, 2019, 9, 496.	1.6	10
88	Thermodynamic study and syntheses of β-SiAlON ceramics. Science in China Series D: Earth Sciences, 2009, 52, 3122-3127.	0.9	9
89	Facile and Economical Preparation of SiAlON-Based Composites Using Coal Gangue: From Fundamental to Industrial Application. Energies, 2015, 8, 7428-7440.	1.6	9
90	Solid wastes utilization in the iron and steel industry in China: towards sustainability. Institutions of Mining and Metallurgy Transactions Section C: Mineral Processing and Extractive Metallurgy, 2017, 126, 41-46.	0.6	8

#	Article	IF	CITATIONS
91	Promoting Effect of Ti Species in MnOx-FeOx/Silicalite-1 for the Low-Temperature NH3-SCR Reaction. Catalysts, 2020, 10, 566.	1.6	8
92	Computational Screening and Synthesis of M (M = Mo and Cu)-Doped CeO ₂ /silicalite-1 for Medium-/Low-Temperature NH ₃ –SCR. Industrial & Engineering Chemistry Research, 2022, 61, 10091-10105.	1.8	8
93	Conductivity properties of Î ² -SiAlON ceramics. Science China Technological Sciences, 2012, 55, 2409-2415.	2.0	7
94	Three-Stage Method Energy–Mass Coupling High-Efficiency Utilization Process of High-Temperature Molten Steel Slag. Metallurgical and Materials Transactions B: Process Metallurgy and Materials Processing Science, 2021, 52, 3004-3015.	1.0	7
95	Investigation of cooling processes of molten slags to develop multilevel control method for cleaner production in mineral wool. Journal of Cleaner Production, 2022, 339, 130548.	4.6	7
96	A Fe-C-Ca big cycle in modern carbon-intensive industries: toward emission reduction and resource utilization. Scientific Reports, 2016, 6, 22323.	1.6	6
97	Highly dispersed MnO _x –FeO _x supported by silicalite-1 for the selective catalytic reduction of NO _x with NH ₃ at low temperatures. Catalysis Science and Technology, 2020, 10, 5525-5534.	2.1	6
98	Thermodynamic modeling of electrolyte solutions by a hybrid ion-interaction and solvation (HIS) model. Calphad: Computer Coupling of Phase Diagrams and Thermochemistry, 2015, 48, 79-88.	0.7	5
99	Long-term leaching behaviours of cement composites prepared by hazardous wastes. RSC Advances, 2018, 8, 27602-27609.	1.7	5
100	Designing Structure–Thermodynamics-Informed Artificial Neural Networks for Surface Tension Prediction of Multi-component Molten Slags. Metallurgical and Materials Transactions B: Process Metallurgy and Materials Processing Science, 2022, 53, 2018-2029.	1.0	4
101	Slag corrosion of gamma aluminium oxynitride. Steel Research = Archiv Für Das Eisenhüttenwesen, 2002, 73, 91-96.	0.2	3
102	Preparation and Numerical Modelling of Ceramic Foam Insulation for Energy Saving in Buildings. , 0, , .		0
103	Experimental Investigation of Vitrification Process for the Disposal of Hazardous Solid Waste Containing Chlorides. Processes, 2022, 10, 526.	1.3	0
104	Mechanistic and Experimental Study of the CuxO@C Nanocomposite Derived from Cu3(BTC)2 for SO2 Removal. Catalysts, 2022, 12, 689.	1.6	0